



# Green synthesis of quinolines via A<sup>3</sup>-coupling by using graphene oxide-supported Brønsted acidic ionic liquid

Shivanand Gajare<sup>1</sup> · Audumbar Patil<sup>1</sup> · Shankar Hangirgekar<sup>1</sup> ·  
Sushilkumar Dhanmane<sup>2</sup> · Gajanan Rashinkar<sup>1</sup>

Received: 19 October 2019 / Accepted: 5 February 2020  
© Springer Nature B.V. 2020

## Abstract

Graphene oxide-supported Brønsted acidic ionic liquid ([GrBenzImi]SO<sub>3</sub>H) has been prepared by covalent grafting of benzimidazole unit in the matrix of graphene oxide followed by reaction with 1,4-butane sultone and hydrochloric acid. [GrBenzImi]SO<sub>3</sub>H has been characterized by various techniques including Fourier transform infrared spectroscopy (FTIR), FT-Raman (FT-Raman spectroscopy), CP-MAS <sup>13</sup>C NMR spectroscopy, thermogravimetric analysis, energy-dispersive X-ray analysis, Brunauer–Emmett–Teller surface area, X-ray diffraction, and transmission electron microscopy. [GrBenzImi]SO<sub>3</sub>H was successfully employed as heterogeneous catalyst in A<sup>3</sup>-coupling reaction of aryl aldehydes, anilines and phenylacetylene for the synthesis of 2,4-disubstituted quinolines using water/ethanol system (1:1) as green medium. [GrBenzImi]SO<sub>3</sub>H could be recycled six times without significant loss in the yield of product.

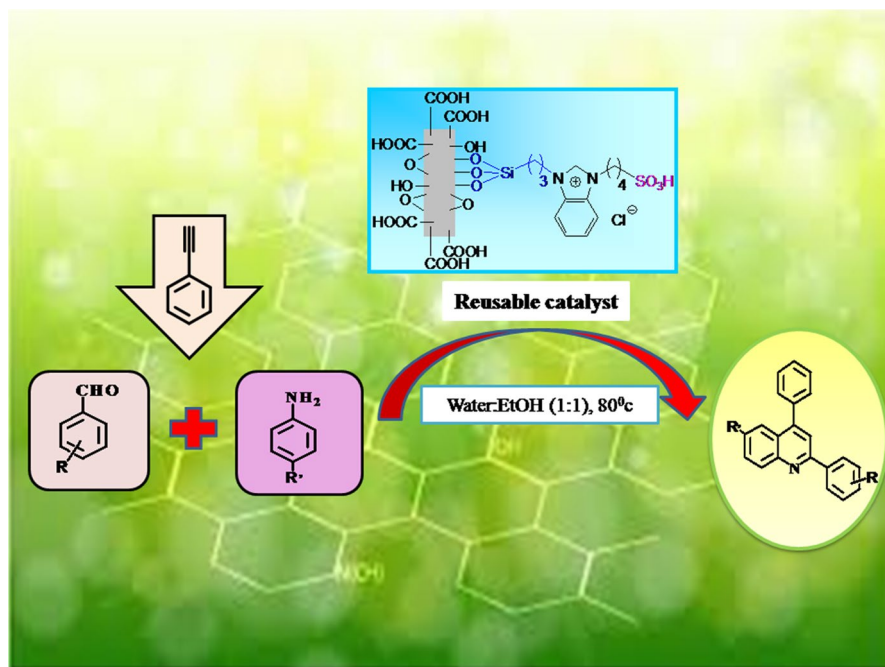
**Electronic supplementary material** The online version of this article (<https://doi.org/10.1007/s11164-020-04099-7>) contains supplementary material, which is available to authorized users.

✉ Gajanan Rashinkar  
gsr\_chem@unishivaji.ac.in  
Sushilkumar Dhanmane  
Sushorganic@gmail.com

<sup>1</sup> Department of Chemistry, Shivaji University, Kolhapur, MS 416004, India

<sup>2</sup> Department of Chemistry, Fergusson College, Pune, MS 411004, India

## Graphic abstract



**Keywords** Brønsted acidic ionic liquid · Graphene oxide · A<sup>3</sup>-coupling · 2,4-disubstituted quinolines · Reusability

## Introduction

Advent of green chemistry principles has spurred extensive interest in developing environmentally benign processes using Brønsted acidic ionic liquids (BAILs) in organic synthesis [1–4]. BAILs circumvent the environmental and personal toxicity concern that are associated with traditional Brønsted acids and offer high thermal stability as well as high acidity accompanied by negligible release of hazardous gases. In addition, their excellent catalytic performance, non-hygroscopic nature, easy separation from reaction medium makes their utilization economically feasible [5–7]. Owing to these properties BAILs have been exploited for various organic transformations such as aza-Michael reaction, Beckmann rearrangement, Pechmann reaction, Mannich reaction, Koch carbonylation, Prin's reaction, Hantzsch reaction [8]. In recent years, great attention has been dedicated to the development of supported BAILs as they offer significant advantages such as high reactivity and facile reusability over homogeneous BAILs. In addition, they can be applied in continuous fixed bed reactors. Owing to these advantages, supported BAILs have been employed in the pharmaceuticals, polymers,

biodiesel as well as in oil refining and petroleum industries [9–12]. A careful insight into heterogeneous BAILs reveals that their catalytic performance depends on the nature of support material [13]. In view of this, various supports such as silica, alumina, zeolites and polystyrene type polymers have been employed for the preparation of supported BAILs [14]. However, despite considerable progress, there is still scope to develop novel supported BAILs especially using nanomaterials as a support.

Nanostructure materials have emerged as attractive supports in the synthesis of heterogeneous catalysts. They offer extraordinary features such as nanosize, large surface-to-volume ratio, and ease of surface functionalization [15]. In the recent years, graphene oxide (GO) has emerged as one of the most promising two-dimensional (2D) nanomaterial that has been widely applied in wide areas including cancer therapy, photocatalysis, organic synthesis, electrochemistry, tissue engineering, imaging, diagnostics, etc. [16–19]. GO possesses unique features such as large surface area, ultrahigh electrical conductivity, excellent mechanical properties, high chemical stability, surface functionalizability, amphiphilicity, fluorescence quenching capacity, surface-enhanced Raman scattering (SERS) property, and amazing aqueous processability. Due to these fascinating properties, GO has emerged as unparallel 2D support in the preparation of heterogeneous catalysts [20]. The recent applications of GO-supported ionic liquid catalysts in the realm of catalysis have demonstrated their tremendous potential in the development of economical, efficient and environmentally benign processes [21].

The efficacious catalytic construction of bio-relevant heterocyclic architectures is still a fascinating endeavor for chemists intending to explore new chemical spaces and to develop more sustainable organic synthesis [22]. Quinolines are privileged heterocyclic scaffolds with wide range of pharmacological properties such as anticancer, antimalarial, antimicrobial, antitubercular, anti-inflammatory, antioxidant, anticonvulsant, and antihypertensive activities [23]. Owing to the wide array of biological activities, methodology of their synthesis has attracted significant attention in the last decade. In line with their increasing relevance, numerous bespoke classical strategies such as classical Skraup [24], Doebner–Miller [25], Friedlander [26], Pfitzinger reactions [27], Conrad–Limpach [28], and Combes synthesis [29] have been explored for their synthesis. However, many of these methods suffer from limitations such as expensive reagents or catalysts, strong acidic conditions, long reaction times, high temperatures and environmentally unfriendly solvents. In recent years,  $A^3$ -coupling reaction between aromatic aldehyde, anilines, and terminal alkynes has been established as a convenient method for synthesis of quinolines [30–32]. However, despite impressive progress, a thrust toward developing a green procedure using a more efficient heterogeneous catalyst is a subject of immense research in organic synthesis.

Based on aforementioned facts and in continuation of our studies related to heterogeneous catalysis [33, 34], herein we report an eco-friendly, efficient, and versatile approach for the synthesis of 2,4-disubstituted quinolines using graphene oxide-supported Brønsted acidic ionic liquid as a catalyst.

## Experimental section

### General remarks

All reactions were carried out under air atmosphere in dried glassware. FTIR spectra were measured with a PerkinElmer one FTIR spectrophotometer. The samples were examined as KBr discs (~5% w/w). Raman spectroscopy was done using a Bruker: RFS 27 spectrometer. The thermogravimetric analysis (TGA) curves were obtained using instrument SDT Q600 V20.9 Build 20 in the presence of static air at linear heating rate of 10 °C/min from 25 to 1000 °C. Elemental analyses were performed in a PerkinElmer 2400, Series II, CHNS/O analyzer and using an energy-dispersive X-ray spectroscopic facility (Hitachi S 4800, Japan).  $^1\text{H}$  NMR and  $^{13}\text{C}$  NMR spectra were recorded with a Bruker Avance (300 MHz for  $^1\text{H}$  NMR and 75 MHz for  $^{13}\text{C}$  NMR) spectrometer using  $\text{CDCl}_3$  solvent and tetramethylsilane as an internal standard. Chemical shifts are expressed in parts per million (ppm) and coupling constants are expressed in hertz (Hz). The CP-MAS  $^{13}\text{C}$  NMR spectrum was recorded with a JEOL-ECX400 type FT-NMR spectrometer. Mass spectra were recorded with a Shimadzu QP2010 gas chromatography–mass spectrometry (GC–MS). The materials were analyzed by TEM using a PHILIPS CM 200 model with 20–200 kV accelerating voltages. Melting points were determined using MEL-TEMP capillary melting point apparatus and are uncorrected. BET (Brunauer–Emmet–Teller) Quantachrome Nova Win surface area analyzer was used for surface area and pore size measurements by  $\text{N}_2$  adsorption–desorption analysis. X-ray powder diffraction (XRD) was taken using a Bruker D2 Phaser. Graphite (**1**) and all other chemicals were obtained from local suppliers and used without further purification. Graphite oxide (**2**) and graphene oxide (GO) (**3**) were synthesized following the literature procedure [35, 36] and reported in our previous work [37].

### Preparation of 3-chloropropyl graphene oxide (**4**)

A mixture of **3** (8.0 g) and (3-chloropropyl)triethoxysilane (10.8 mL, 45 mmol) in xylene (50 mL) was refluxed in an oil bath. After 24 h, the mixture was cooled, and the residue was separated by centrifugation, washed with THF ( $3 \times 5$  mL), and dried under vacuum at room temperature to afford 3-chloropropyl graphene oxide (**4**).

IR (KBr, thin film):  $\nu = 3437, 2945, 2885, 2375, 1698, 1426, 995, 792, 682\text{ cm}^{-1}$ ; Raman:  $\nu = 3036, 2129, 1974, 1597, 1293\text{ cm}^{-1}$ ; Loading: 0.12 mmol of functional group per gram of **4**.

### Preparation of [GrBenzImi] (**6**)

A mixture of **4** (8.0 g) and sodium salt of benzimidazole (**5**) (2 g, 15 mmol) in benzene (50 mL) was heated at 80 °C in an oil bath. After 24 h, the solid was separated by centrifugation, washed with benzene ( $3 \times 50$  mL), MeOH ( $3 \times 50$  mL),  $\text{CH}_2\text{Cl}_2$  ( $3 \times 50$  mL), and dried under vacuum at 50 °C for 24 h to afford [GrBenzImi] (**6**).

IR (KBr, thin film):  $\nu$  = 3410, 2922, 2856, 1670, 1565, 1405, 1322, 1097, 1023, 467 cm<sup>-1</sup>. Raman:  $\nu$  = 3064, 2714, 2117, 1594, 1296 cm<sup>-1</sup>. Elemental analysis observed: %C 68.57, %H 0.25, % N 5.59. Loading: 0.47 mmol functional group per gram of **6**.

### Preparation of [GrBenzImi]SO<sub>3</sub>H (**7**)

A mixture of **6** (10.0 g) and 1,4-butane sultone (2.5 g, 18 mmol) in toluene (50 mL) was heated at 100 °C in an oil bath for 6 h. Afterward, the mixture was treated with conc. HCl (3 mmol, 36% w/w) and allow to stand at room temperature for 24 h, and washed with the diethyl ether (3 × 50 mL) and dried under vacuum at 50 °C for 24 h to afford [GrBenzImi]SO<sub>3</sub>H (**7**).

FTIR (KBr, thin film):  $\nu$  = 3410, 2922, 2856, 1670, 1565, 1188, 1034 cm<sup>-1</sup>; Raman:  $\nu$  = 3064, 2774, 2136, 1599, 1294 cm<sup>-1</sup>. Elemental analysis observed: %C 68.57, % O 19.43, % Si 2.87, % N 5.59, % Cl 2.91, % S 0.38 and % H 0.25. Loading of SO<sub>3</sub>H: 0.12 mmol functional group per gram of **7**.

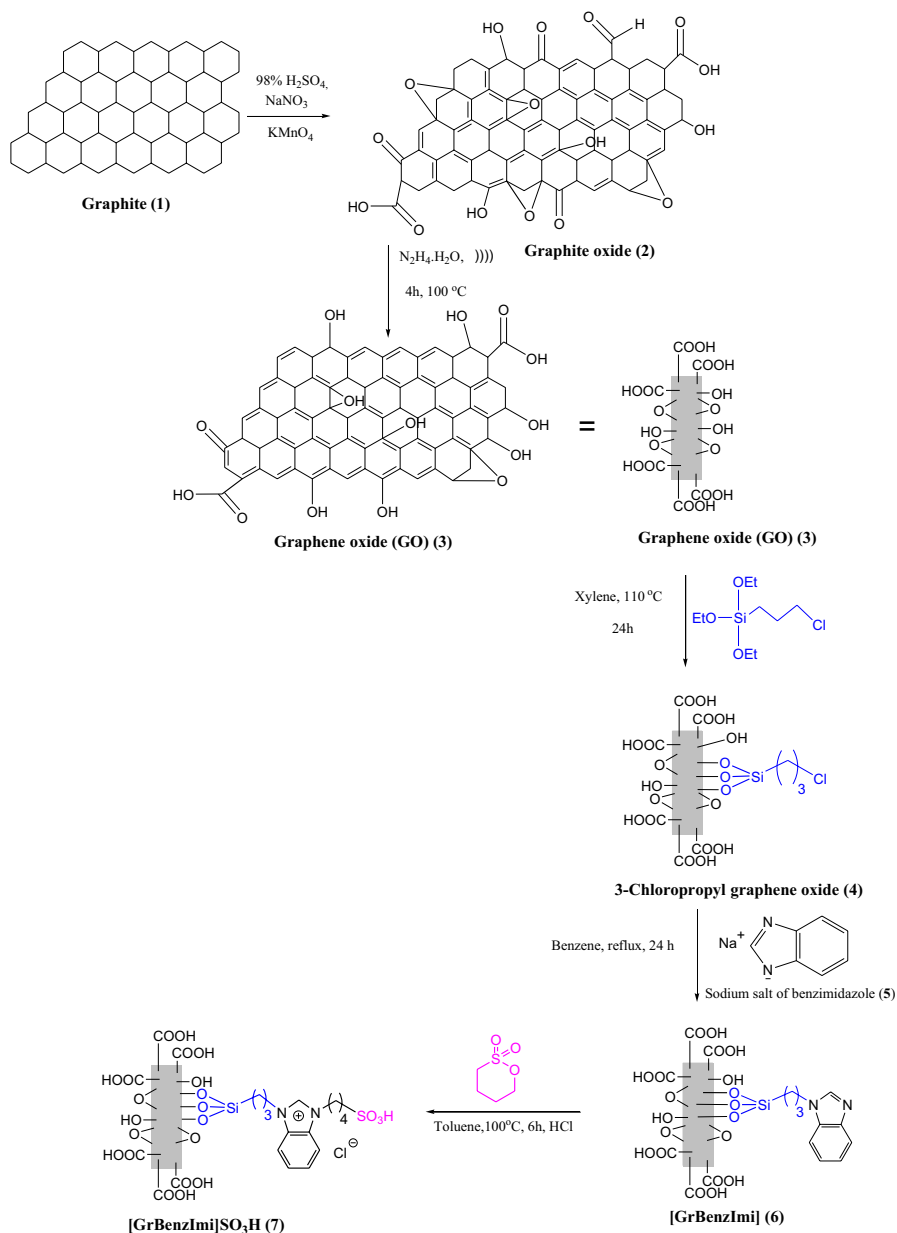
### General method for synthesis of 2,4-disubstituted quinolines

A mixture of aryl aldehyde (1 mmol), aniline (1 mmol), phenylacetylene (1 mmol), and [GrBenzImi]SO<sub>3</sub>H (**7**) (50 mg) in water/ethanol (1;1) solvent system (3 mL) was stirred at 80 °C. After completion of the reaction as monitored by the TLC, the reaction mixture was centrifuged to remove **7**. Evaporation of solvent in vacuo followed by column chromatography over silica gel using petroleum ether/ethyl acetate afforded pure products.

## Results and discussion

The preparation of graphene oxide-supported Bronsted acidic ionic liquid phase catalyst is outlined in Scheme 1. Initially, purified graphite (**1**) was oxidized to graphite oxide (**2**) following modified Hummers and Offeman's method [35, 36]. The ultrasound-mediated exfoliation of **2** using hydrazine hydrate in aqueous medium afforded graphene oxide (GO) (**3**) [37] which on further treatment with (3-chloropropyl)triethoxysilane afforded 3-chloropropyl graphene oxide (**4**). The synthetically fertile chloro group in **4** allowed introduction of ionic liquid-like group in the GO matrix through quaternization with sodium salt of benzimidazole (**5**) to yield precursor acronymed as [GrBenzImi] (**6**). Finally, the acid treatment of **6** with 1,4-butane sultone and hydrochloric acid afforded the desired GO-supported Bronsted acidic ionic liquid acronymed as [GrBenzImi]SO<sub>3</sub>H (**7**).

Fourier transform infrared (FTIR), FT-Raman, and cross-polarization magic angle spinning (CP-MAS) <sup>13</sup>C NMR spectroscopy were used to monitor the reactions involved in the preparation of [GrBenzImi]SO<sub>3</sub>H (**7**). The FTIR spectrum of 3-chloropropyl graphene oxide (**4**) displayed peaks at 3437 (O–H stretching), 2885 (C–H stretching), 995 (Si–O stretching) and 682 cm<sup>-1</sup> (C–Cl stretching)



**Scheme 1** Preparation of [GrBenzImi]SO<sub>3</sub>H (7)

[38, 39] (Fig. 1c). The quaternization of **4** with sodium salt of benzimidazole (**5**) was monitored by FTIR spectroscopy. The vanishing of C–Cl stretching peak at  $682\text{ cm}^{-1}$  and appearance of bands at  $1565$  (C=N stretching of benzimidazolium ring),  $1670$  (C=C stretching of benzimidazolium) and  $2922\text{ cm}^{-1}$  (C–H stretching

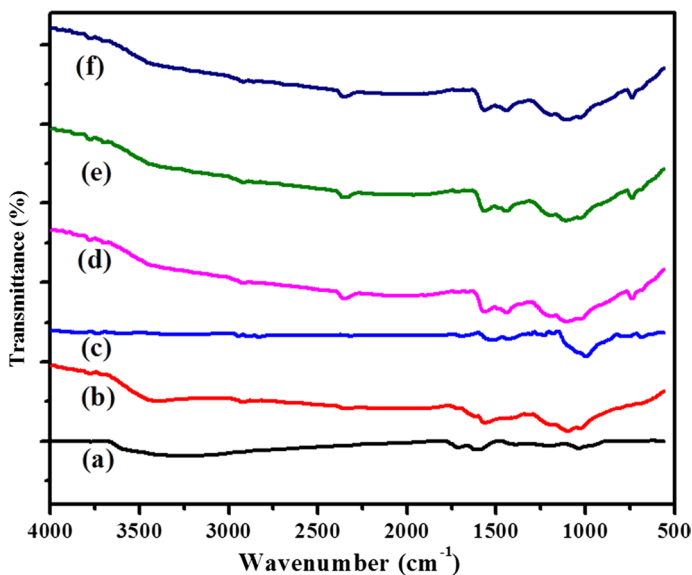


**Fig. 1** FTIR spectra of (a) Graphite oxide (**2**); (b) Graphene oxide (**3**); (c) 3-Chloropropyl graphene oxide (**4**); (d) [GrBenzImi] (**6**); (e) [GrBenzImi]SO<sub>3</sub>H (**7**); (f) Reused [GrBenzImi]SO<sub>3</sub>H (**7**)

of benzimidazolium) demonstrated successful formation of **6** via quaternization (Fig. 1d). The formation of [GrBenzImi]SO<sub>3</sub>H (**7**) was confirmed on the basis of characteristic peaks at 1188 cm<sup>-1</sup> (asymmetric stretching of S=O of sulfonate group) and 1034 cm<sup>-1</sup> (symmetric stretching of S=O of sulfonate group) (Fig. 1e) [40, 41]. Another promising technique to study structural defects and structural modifications in graphene-based material is Raman spectroscopy. The Raman analysis of [GrBenzImi] (**6**) (Fig. 2a) and [GrBenzImi]SO<sub>3</sub>H (**7**) (Fig. 2b) displayed two major characteristic bands, assigned as D and G bands. The D band results from vibrations due to the structural imperfections that are caused by the attachment of oxygenated groups on the *sp*<sup>3</sup>-hybridized graphitic sheet carbons basal plane and disordered lattices, while the G band arises due to vibration of the *sp*<sup>2</sup>-hybridized carbon atoms in graphene lattices and the first-order scattering from the doubly degenerate *E*<sub>2g</sub> phonon modes of graphite as well as bond stretching of *sp*<sup>2</sup> carbon pairs in both rings and chains of graphene skeleton. The D and G band peaks in **6** were observed at 1296 cm<sup>-1</sup> and 1594 cm<sup>-1</sup>, respectively. The D and G band peaks for **7** were displayed at 1296 cm<sup>-1</sup> and 1599 cm<sup>-1</sup> indicating that position of the D band is almost the same before and after the chemical modifications but G band shows slight redshift due to increasing strain by sulfonic group attached on the surface of graphene oxide [42, 43]. In addition, **7** shows higher intensity of D band (0.014) than G band (0.012) due to introduction of benzimidazolium group in the GO matrix revealing the formation of **7** [44]. Finally, the CP-MAS <sup>13</sup>C NMR of **7** displayed signals at δ 193 (C=O groups of graphene), 169 (O=C–O), 101 (O–C–O), 130 (graphitic *sp*<sup>2</sup>–C), 70 (C–OH), 62 (epoxide), 153 (*s*, benzimidazolium C<sub>2</sub>), 152 (*s*, benzimidazolium

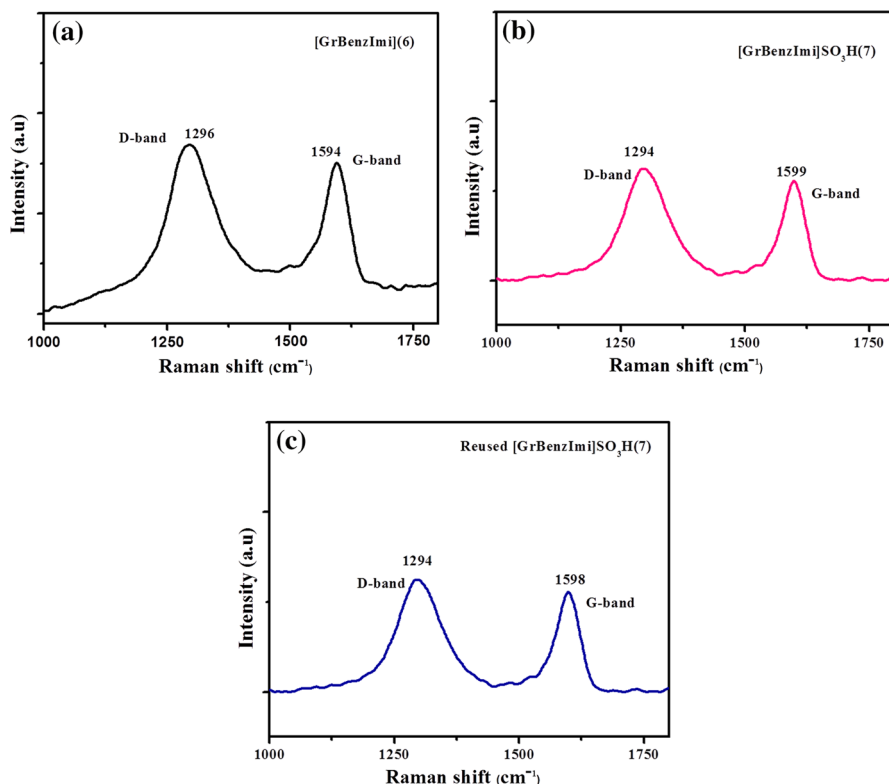


**Fig. 2** **a** Raman spectra of [GrBenzImi]Cl (**6**). **b** Raman spectra of [GrBenzImi]SO<sub>3</sub>H (**7**). **c** Raman spectra of reused [GrBenzImi]SO<sub>3</sub>H (**7**)

C<sub>4</sub>), 120 (*s*, benzimidazolium C<sub>5</sub>), 49 (*s*, 1C, =N–CH<sub>2</sub>CH<sub>2</sub>–CH<sub>2</sub>), 28 (*s*, 1C, =N–CH<sub>2</sub>CH<sub>2</sub>–CH<sub>2</sub>), 8 (*s*, 1C, –CH<sub>2</sub>Si) confirming the formation of **7**.

Thermogravimetric analysis (TGA) was employed to study of thermal stability of [GrBenzImi]SO<sub>3</sub>H (**7**) over the temperature range of 25–1000 °C at heating rate of 10 °C/min (Fig. 3). The TGA curve displayed three major weight losses. The initial weight loss of 1.7% below 200 °C is due to release of physically adsorbed water. The second key weight loss of 38.7% up to 535 °C is attributed to loss of labile oxygen-containing groups such as CO and CO<sub>2</sub> [45] as well as liberation of SO<sub>3</sub>H group [46] and surface-bound organic scaffolds from GO surface [47]. The major weight loss of 49.2% up to 754 °C ascribed to complete combustion of GO and carbon skeleton.

The elemental mapping by energy-dispersive X-ray spectroscopic analysis (EDX) of [GrBenzImi]SO<sub>3</sub>H (**7**) revealed carbon and oxygen as the major elements which are attributed to GO skeleton whereas displayed minor peaks for silicon and sulfur. The presence of sulfur in its respective energy position at 2.2–2.3 keV also supports the formation of **7** [48]. Further, the quantification of



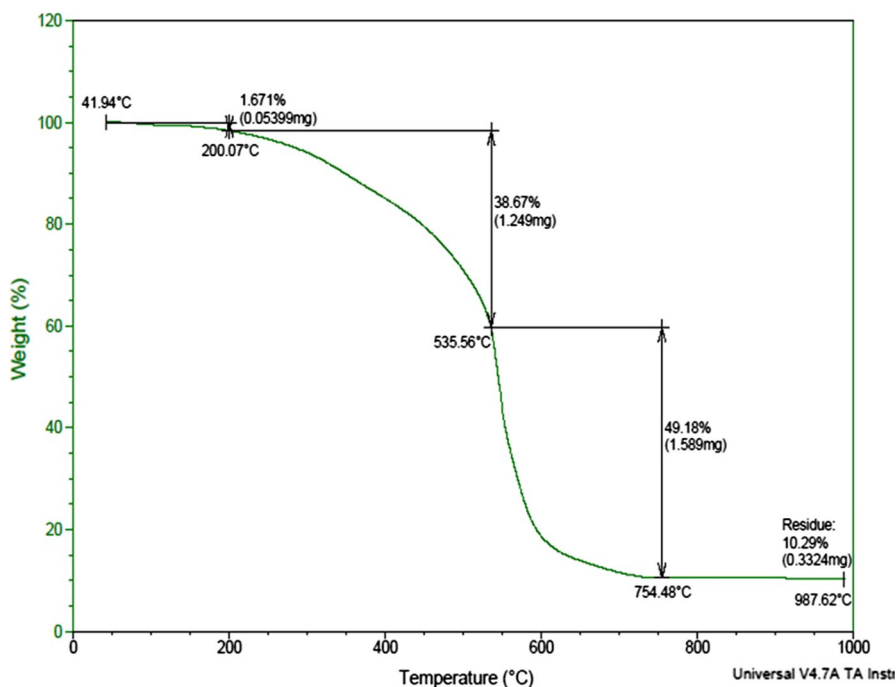


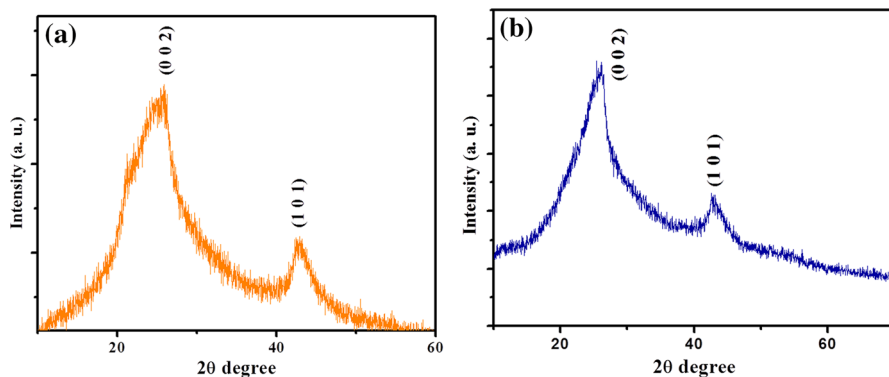
Fig. 3 TGA curve of [GrBenzImi]SO<sub>3</sub>H (7)

SO<sub>3</sub>H group in **7** was performed by employing volumetric titration analysis [49] and was found to be 0.12 mmol per gram of **7**.

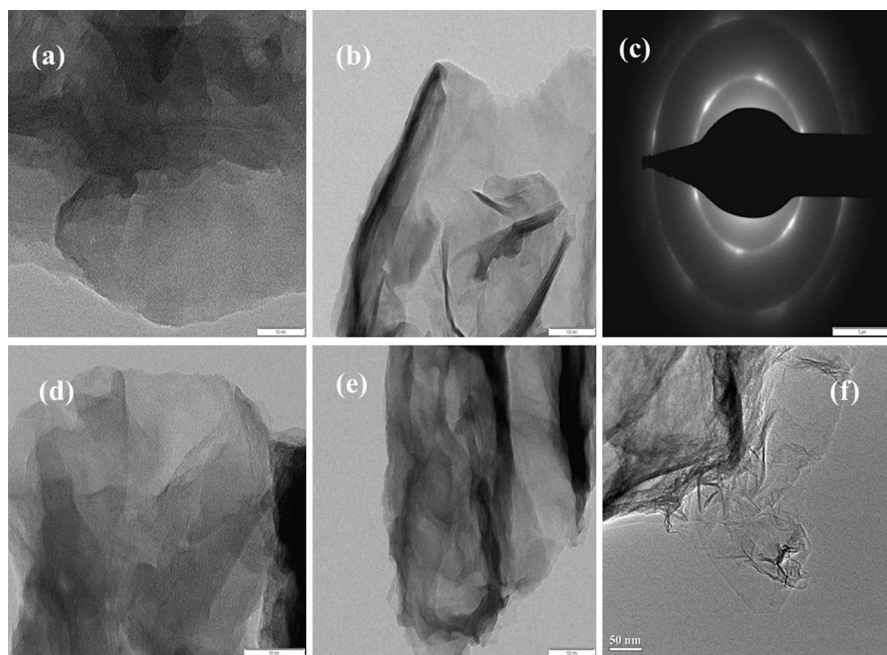
The surface area and textural properties of GO (**3**) and [GrBenzImi]SO<sub>3</sub>H (**7**) were analyzed by Brunauer–Emmett–Teller (BET) using nitrogen. The **7** showed BET surface area of 49.72 m<sup>2</sup>/g with the average pore diameter of 19 Å. The surface area, pore volume, and pore size of **7** were significantly lower than that of pristine GO (**3**) (77 m<sup>2</sup>/g, 23 Å) indicating loss of micropores due to substantial grafting of organic moieties on the matrix of graphene oxide [50].

The evidence for retention of crystal structure of GO (**3**) (Fig. 4a) in [GrBenzImi]SO<sub>3</sub>H (**7**) (Fig. 4b) was further investigated by X-ray diffraction (XRD). The diffractograms of GO (**3**) and **7** displayed two main characteristic peaks at  $2\theta$  values 26.0° and 43.3° which are attributed to (002) and (101) reflections of graphitized carbon. Thus XRD analysis revealed that the structure of pristine GO was retained in **7** even after multi-step functionalization [51]. In addition, the peak range of  $2\theta$  = 13°–16°, which is due to the presence of benzimidazolium groups on the graphene oxide sheets was also observed [52].

The surface morphology of GO (**3**) and [GrBenzImi]SO<sub>3</sub>H (**7**) were studied by transmission electron microscopy (TEM). The TEM image of **7** (Fig. 5a–c) and pristine GO (**3**) (Fig. 5f) displayed agglomerated, wrinkled and folded sheet-like structure which is inconsistent with graphene oxide structure and crumpling features with twisted nanosheets in disordered phase [53]. The GO nanosheets carry immobilized



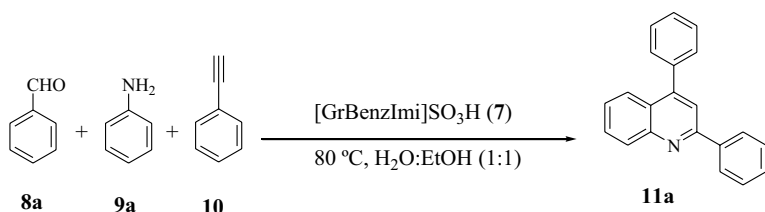
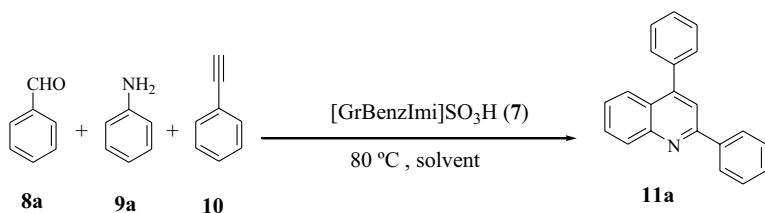
**Fig. 4** **a** XRD of graphene oxide (GO) (3). **b** XRD of [GrBenzImi]SO<sub>3</sub>H (7)



**Fig. 5** TEM images of **a–c** [GrBenzImi]SO<sub>3</sub>H (7) with SAED pattern; **d, e** reused [GrBenzImi]SO<sub>3</sub>H (7); **f** TEM image of graphene oxide (GO) (3)

spherical dense spots which are attributed to the presence of benzimidazolium group and SO<sub>3</sub>H group. The selected area electron diffraction (SAED) pattern exhibit diffused ring pattern that persuades amorphous nature of GO nanosheets [54].

In order to optimize the reaction conditions, a model reaction between benzaldehyde (**8a**; 1 mmol), aniline (**9a**; 1 mmol), and phenyl acetylene (**10**; 1.0 mmol) in the presence of [GrBenzImi]SO<sub>3</sub>H (7) was carried out at 80 °C for the synthesis of 2,4-disubstituted quinolines (Scheme 2). Initially, the effect of various solvents

**Scheme 2** [GrBenzImi]SO<sub>3</sub>H (7) catalyzed synthesis of 2,4-disubstituted quinolines**Table 1** Optimization of solvent in synthesis of 2,4-disubstituted quinolines

Entry	Solvent	Time (min)	Yield <sup>a</sup> (%)
1	Water	20	55
2	DCM	25	76
3	THF	20	78
4	Acetonitrile	20	72
5	Ethanol	15	92
6	Methanol	15	86
7	Toluene	25	68
8	Water/ethanol (1:1)	18	93

Reaction condition: benzaldehyde (1 mmol), aniline (1 mmol), phenyl acetylene (1 mmol), solvent (3 mL)

<sup>a</sup>Isolated yields after chromatography

on the model reaction was investigated in the presence of **7** at 80 °C (Table 1). The reaction afforded poor yield of **11a** in water (Table 1, entry 1), whereas better yields were obtained in polar aprotic solvents such as dichloromethane (DCM), tetrahydrofuran (THF) and acetonitrile (Table 1, entries 2–4). Further, moderate yield of **11a** was obtained in nonpolar solvent such as toluene (Table 1, entry 7). Moreover, better yields were achieved in polar protic solvents like methanol and ethanol (Table 1, entries 5–6). Among all the screened solvents, combination of water and ethanol (1:1) system furnished the highest yield **11a** (Table 1, entry 8). Therefore, water/ethanol (1:1) system was chosen as the solvent for further studies. Initially a control reaction was carried out by using GO (**3**) and [GrBenzImi] (**6**). The reaction could not be initiated by using **3** and **6** in spite of using high



aldehydes (**8**), substituted anilines (**9**) and phenylacetylene (**10**). The results are summarized in Table 3. In all the cases, reactions proceeded smoothly affording the desired 2,4-disubstituted quinolines in good to excellent yields. It is worth mentioning that electronic effect of substituents in anilines has influence on the yields of products. Anilines with electron-donating substituents such as 4-methoxy aniline (Table 3, entry **9c**), and 4-methyl aniline (Table 3, entry **9g**) reacted more efficiently than anilines with electron-withdrawing substituents such as 4-chloro aniline (Table 3, entry **9b**) and 4-nitro aniline (Table 3, entry **9f**).

A plausible mechanism of [GrBenzImi]SO<sub>3</sub>H (**7**) catalyzed synthesis of 2,4-disubstituted quinolines is outlined in Scheme 3. Initially, **7** activates the carbonyl group of aldehyde through hydrogen bonding which facilitated Knoevenagel condensation with aniline affording aldimine intermediate (**A**) via removal of water molecule. Further, addition of phenylacetylene to **A** forms the propargylamine intermediate (**B**) which undergoes cyclization to form the dihydroquinoline intermediate (**C**). Finally, **C** is subsequently oxidized by O<sub>2</sub> in air to give the desired 2, 4-disubstituted quinoline (**D**) [55–57].

The hot filtration test was carried out to confirm heterogeneous nature of [GrBenzImi]SO<sub>3</sub>H (**7**) by using the model reaction. In this test, a mixture of **7** (50 mg), benzaldehyde (**8a**; 1 mmol) aniline (**9a**; 1 mmol) and phenylacetylene (**10**; 1 mmol) in water/ethanol (1:1) (3 mL) was heated at 80 °C. The **7** was separated from the hot reaction mixture when 50% conversion was accomplished (GC). The reaction was continued with the filtrate for further 8 h. There was no increase in the yield of the product beyond 50% even after 8 h confirming the heterogeneous nature of **7**.

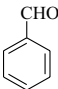
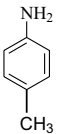
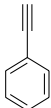
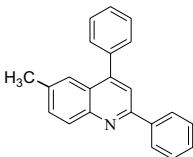
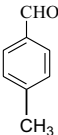
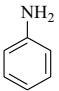
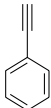
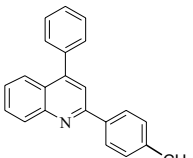
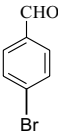
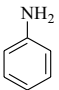
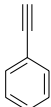
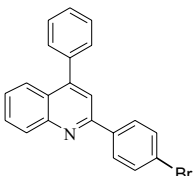
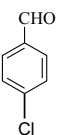
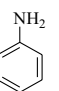
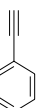
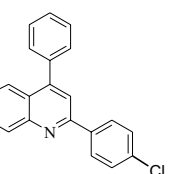
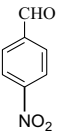
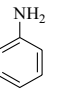
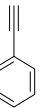
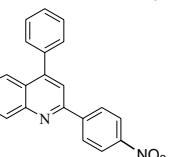
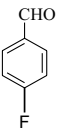
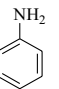
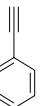
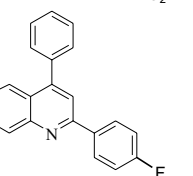
From the green chemistry point of view, the reusability is one of the significant facets of heterogeneous catalyst to determine efficient recovery and reuse of the catalyst with their dynamic life span. Thus, the recovery and reusability of [GrBenzImi]SO<sub>3</sub>H (**7**) investigated by employing model reaction (Fig. 6). In brief, after reaction was completed, the **7** was isolated from reaction mixture by centrifugation. The recovered **7** was washed several times with water/ethanol solvent system, dried in vacuum at room temperature and used directly for the next cycle. The recovered catalyst could be reused for six times without significant decrease in the yield of the products. Further, the stability of recycled catalyst **7** was studied by FTIR spectroscopy, FT-Raman spectroscopy, EDX and TEM analysis. It is noteworthy to mention that, the FTIR (Fig. 1f) and FT-Raman (Fig. 2c) spectra of reused **7** still retain the prominent peak pattern of the **7**. The EDX mapping of **7** after six catalytic cycles confirmed the integrity of the recycled catalyst. Moreover, TEM analysis of fresh (Fig. 5a–c) and reused **7** (Fig. 5d, e) designates that morphology is preserved even after six successive runs. The results of FTIR, FT-Raman, EDX and TEM analysis of fresh and reused **7** confirmed that the structural rigidity and main characteristics of complex remain conserved, demonstrating stability of **7** after six consecutive runs.

To demonstrate the importance of [GrBenzImi]SO<sub>3</sub>H (**7**) in comparison with other reported traditional methods, we have summarized previous report for synthesis of quinolines in Tables 4 and 5. The comparison of results (Table 5.) clearly

**Table 3** [GrBenzImi]SO<sub>3</sub>H (7) catalyzed synthesis of 2,4-disubstituted quinolines

	<b>8a-l</b>	<b>9a-l</b>	<b>10</b>			<b>11a-l</b>
Entry	Aldehydes (8)	Anilines (9)	Phenyl acetylene (10)	Product (11)	Time (Min)	Yield <sup>a</sup> (%)
a					18	93
b					15	78
c					25	90
d					22	88
e					20	83
f					20	80

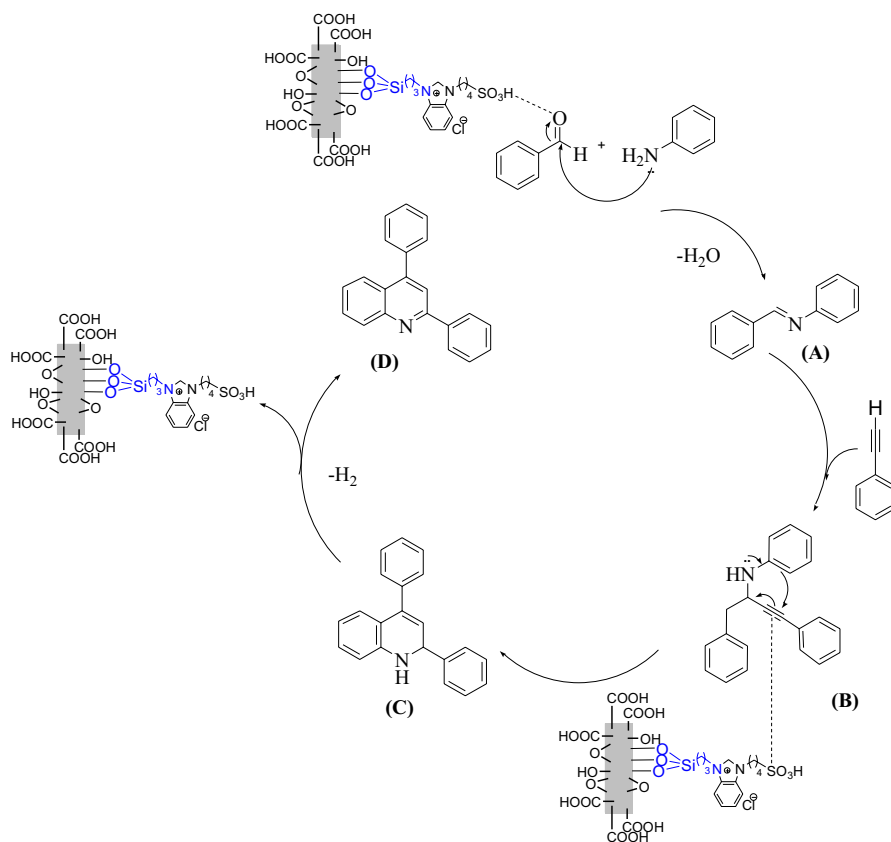
**Table 3** (continued)

Entry	Aldehydes (8)	Anilines (9)	Phenyl acetylene (10)	Product (11)	Time (Min)	Yield <sup>a</sup> (%)
g					22	89
h					20	88
i					18	90
j					15	87
k					17	89
l					26	82

Reaction condition: benzaldehyde (1 mmol), aniline (1 mmol), phenyl acetylene (1 mmol), solvent water/ethanol (1:1) (3 mL); [GrBenzImi]SO<sub>3</sub>H (**7**) (50 mg)

<sup>a</sup>Isolated yields after chromatography

persuades that **7** is a superior catalyst in terms of catalyst loading and reaction time as compared to the reported catalyst.



**Scheme 3** Plausible mechanism for the synthesis of 2,4-disubstituted quinolines using [GrBenzImi]SO<sub>3</sub>H (7)

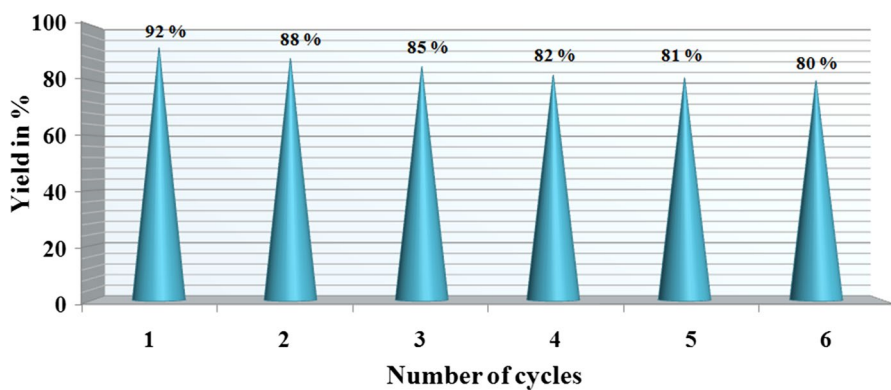


**Fig. 6** Reusability of [GrBenzImi]SO<sub>3</sub>H (7) in the synthesis 2,4-disubstituted quinolines



**Table 4** Comparison of advantages and disadvantages between the reported method and traditional methods for the synthesis of quinolines

Traditional methods	Disadvantages	Reference
Skraup reaction Doebner–von Miller synthesis, Doebner synthesis, Combes synthesis, Pfiz- inger synthesis, and Friedländer synthesis	(1) Toxic and complex starting materials (2) Multiple reaction steps (3) Low efficiency, (4) long time reaction and (5) Poor regioselectivity, thus giving relatively simple products with limited substitution patterns especially for those bearing 2,4-disubstituted functional group moieties. These existing drawbacks greatly hinder their application and subsequent derivatization since the 2,4-disubstituted quinoline frame- work is commonly found in numerous natural products and pharmaceutical drugs as well as in biologically active compounds	[58]
Reported method	Advantages	
Present work	Good yields, simple workup procedure, one-pot synthesis, short reaction time, use of environmentally benign solvent and efficient recyclability of the catalyst	

**Table 5** Comparison of this work with literature results for synthesis of 2,4-disubstituted quinolines catalyzed by various catalysts

Entry	Catalyst	Solvent	Temperature	Time (min)	Yield (%)
1	NbCl <sub>5</sub>	Acetonitrile	Reflux	1440	74
2	Nano AMA	Acetonitrile	Reflux	45	90
3	FeCl <sub>3</sub>	1,2-Dichloroethane	Reflux	720	93
4	Fe(OTf) <sub>3</sub> (5%)	Solvent free	100 °C	180	71
5	1 wt% CeO <sub>2</sub> -TiO <sub>2</sub>	None	80 °C	90	95
6	BF <sub>3</sub> •E <sub>2</sub> O	Toluene	Reflux	240	88
7	Yb(Pfb) <sub>3</sub>	Toluene	Reflux	1440	82
8	Yb(Pfb) <sub>3</sub>	CH <sub>2</sub> Cl <sub>2</sub>	35 °C	2880	10
9	AgNTf <sub>2</sub> /HOTf	Toluene	80 °C	1440	90
10	InCl <sub>3</sub>	Toluene	Reflux	1440	90
11	In/HCl	Water	Reflux	1080	72
12	I <sub>2</sub>	MeNO <sub>2</sub>	Reflux	720	61
13	AuCl <sub>3</sub> /CuBr	Methanol	rt	23,280	55
14	AlCl <sub>3</sub>	None	110 °C	2880	Trace
15	ZnCl <sub>2</sub>	None	110 °C	2880	Trace
16	Present work [GrBenz- zImi] SO <sub>3</sub> H (7)	Water/EtOH (1:1)	80 °C	18	93

## Conclusion

In conclusion, we have reported a graphene oxide-supported Bronsted acidic ionic liquid [GrBenzImi]SO<sub>3</sub>H (7) catalyst. The catalyst 7 was thoroughly characterized by FTIR, FT-Raman, CP-MAS <sup>13</sup>C NMR spectroscopy, XRD, TEM, TGA, EDX and BET analysis. [GrBenzImi]SO<sub>3</sub>H was successfully employed as a heterogeneous catalyst with outstanding activity in A<sup>3</sup>-coupling reaction of aryl aldehydes, anilines, and phenylacetylene for the synthesis of 2,4-disubstituted quinolines. The protocol offers several striking advantages such as good yields, simple workup procedure, short reaction time, use of environmentally benign solvent and efficient recyclability of the catalyst.

**Acknowledgements** We gratefully acknowledge Indian Institute of Bombay (IITB), North-Eastern Hill University Shillong (NEHU), Indian Institute of Technology, Madras (IITM) for providing spectral facilities and Shivaji University Kolhapur for providing financial assistance and Golden Jubilee Research Fellowship (GJRF).

## Compliance with ethical standards

**Conflict of interest** The authors declare that they have no conflict of interest.

## References

1. E. Doustkhah, J. Lin, S. Rostamnia, C. Len, R. Luque, X. Luo, Y. Bando, K.C.-W. Wu, J. Kim, Y. Yamauchi, Y. Ide, *Chem. Eur. J.* **25**, 1614 (2019)
2. L.-Y. Xie, S. Peng, L.-H. Lu, J. Hu, W.-H. Bao, F. Zeng, Z. Tang, X. Xu, W.-M. He, *ACS Sustain. Chem. Eng.* **6**, 7989 (2018)
3. C. Wu, L.-H. Lu, A.-Z. Peng, G.-K. Jia, C. Peng, Z. Cao, Z. Tang, W.-M. He, X. Xu, *Green Chem.* **20**, 3683 (2018)
4. L.-H. Lu, Z. Wang, W. Xia, P. Cheng, B. Zhang, Z. Cao, W.-M. He, *Chin. Chem. Lett.* **30**, 1237 (2019)
5. J.H. Clark, *Acc. Chem. Res.* **35**, 791 (2002)
6. L.M. Gilbertson, J.B. Zimmerman, D.L. Plata, J.E. Hutchison, P.T. Anastas, *Chem. Soc. Rev.* **44**, 5758 (2015)
7. M. Vafaezadeh, H. Alinezhad, *J. Mol. Liq.* **218**, 95 (2016)
8. R. Ratti, *Adv. Chem.* **2014**, 1 (2014)
9. A. Riisager, R. Fehrmann, M. Haumann, P. Wasserscheid, *Eur. J. Inorg. Chem.* **2006**, 695 (2006)
10. G. Busca, *Chem. Rev.* **107**, 5366 (2007)
11. A.F. Lee, J.A. Bennett, J.C. Manayil, K. Wilson, *Chem. Soc. Rev.* **43**, 7887 (2014)
12. H.R. Shaterian, A. Hosseini, *Res. Chem. Intermed.* **40**, 3011 (2014)
13. H.-P. Steinrück, P. Wasserscheid, *Catal. Lett.* **145**, 380 (2015)
14. R. Skoda-Földes, *Molecules* **19**, 8840 (2014)
15. L.L. Chng, N. Erathodiyil, J.Y. Ying, *Acc. Chem. Res.* **46**, 1825 (2013)
16. A. Ramazani, M. Abrvash, S. Sadighian, K. Rostamizadeh, M. Fathi, *Res. Chem. Intermed.* **44**, 7891 (2018)
17. P. Das, S. Ganguly, S. Banerjee, N.C. Das, *Res. Chem. Intermed.* **45**, 3823 (2019)
18. Y. Chen, C. Tan, H. Zhang, L. Wang, *Chem. Soc. Rev.* **44**, 2681 (2015)
19. H.Y. Hafeez, S.K. Lakhera, P. Karthik, M. Anpo, B. Neppolian, *Appl. Surf. Sci.* **449**, 772 (2018)
20. R. Garg, N.K. Dutta, N.R. Choudhury, *Nanomaterials* **4**, 267 (2014)
21. H.D. Hanoon, E. Kowsari, M. Abdouss, H. Zandi, M.H. Ghasemi, *Res. Chem. Intermed.* **43**, 1751 (2017)
22. P. Marion, B. Bernela, A. Piccirilli, B. Estrine, N. Patouillard, J. Guilbot, F. Jérôme, *Green Chem.* **19**, 4973 (2017)
23. S. Narwal, S. Kumar, P.K. Verma, *Res. Chem. Intermed.* **43**, 2765 (2017)
24. R.H.F. Manske, M. Kukla, *Org. React.* **7**, 59 (1953)
25. S.E. Denmark, S. Venkatraman, *J. Org. Chem.* **71**, 1668 (2006)
26. P. Friedlander, C.F. Gohring, *Ber* **16**, 1833 (1883)
27. J.A. Knight, H.K. Porter, P.K. Calaway, *J. Am. Chem. Soc.* **66**, 1893 (1944)
28. R.H. Reitsema, *Chem. Rev.* **43**, 47 (1948)
29. F.W. Bergstrom, *Chem. Rev.* **35**, 156 (1944)
30. Y. Zhang, P. Li, L. Wang, *J. Heterocycl. Chem.* **48**, 153 (2011)
31. Y. Kuninobu, Y. Inoue, K. Takai, *Chem. Lett.* **36**, 1422 (2007)
32. H.Z. Sueda Huma, R. Halder, S.S. Kalra, J. Das, J. Iqbal, *Tetrahedron Lett.* **43**, 6485 (2002)
33. R. Kurane, J. Jadhav, S. Khanapure, R. Salunkhe, G. Rashinkar, *Green Chem.* **15**, 1849 (2013)
34. S. Khanapure, M. Jagadale, R. Salunkhe, G. Rashinkar, *Res. Chem. Intermed.* **42**, 2075 (2016)
35. W.S. Hummers, R.E. Offeman, *J. Am. Chem. Soc.* **80**, 1339 (1958)
36. M. Fang, K. Wang, H. Lu, Y. Yang, S. Nutt, *J. Mater. Chem.* **19**, 7098 (2009)
37. S. Gajare, A. Patil, D. Kale, P. Bansode, P. Patil, G. Rashinkar, *Catal. Lett.* **150**, 243 (2019)
38. H. Naeimi, Z. Ansarian, *Inorg. Chim. Acta* **466**, 417 (2017)
39. C.Y. Lee, Q.V. Le, C. Kim, S.Y. Kim, *Phys. Chem. Chem. Phys.* **17**, 9369 (2017)
40. K. Miyatake, H. Iyotani, K. Yamamoto, E. Tsuchida, *Macromolecules* **29**, 6969 (1996)
41. R. Langner, G. Zundel, *J. Phys. Chem.* **99**, 12214 (1995)
42. J. Ji, G. Zhang, H. Chen, S. Wang, G. Zhang, F. Zhang, X. Fan, *Chem. Sci.* **2**, 484 (2011)
43. T.M.G. Mohiuddin, A. Lombardo, R.R. Nair, A. Bonetti, G. Savini, R. Jalil, N. Bonini, D.M. Basko, C. Galiotis, N. Marzari, K.S. Novoselov, A.K. Geim, A.C. Ferrari, *Phys. Rev. B* **79**, 205433 (2009)
44. A.C. Ferrari, J.C. Meyer, V. Scardaci, C. Casiraghi, M. Lazzeri, F. Mauri, S. Piscanec, D. Jiang, K.S. Novoselov, S. Roth, A.K. Geim, *Phys. Rev. Lett.* **97**, 187401 (2006)

45. S.H. Lee, D.R. Dreyer, J. An, A. Velamakanni, R.D. Piner, S. Park, Y. Zhu, S.O. Kim, C.W. Bielawski, R.S. Ruoff, *Macromol. Rapid Commun.* **31**, 281 (2010)
46. S. Ayyaru, Y.H. Ahn, *J MembSci.* **525**, 210 (2017)
47. M.G. Rabbani, H.M. El-Kaderi, *Chem. Mater.* **24**, 1511 (2012)
48. V. Panwar, K. Cha, J.O. Park, S. Park, *Sens. Actuators B Chem.* **161**, 460 (2011)
49. M. Saikia, L. Saikia, *RSC Adv.* **6**, 15846 (2016)
50. Q. Dong, X. Zhuang, Z. Li, B. Li, B. Fang, C. Yang, H. Xie, F. Zhang, X. Feng, *J. Mater. Chem. A* **3**, 7767 (2015)
51. L. Jiao, Y. Hu, H. Ju, C. Wang, M.-R. Gao, Q. Yang, J. Zhu, S.-H. Yu, H.L. Jiang, *J. Mater. Chem. A* **5**, 23170 (2017)
52. W. Ai, W. Zhou, Z. Du, Y. Du, H. Zhang, X. Jia, L. Xie, M. Yi, T. Yu, W. Huang, *J. Mater. Chem.* **22**, 23439 (2012)
53. Q. Huang, L. Zhou, X. Jiang, Y. Zhou, H. Fan, W. Lang, *A.C.S. Appl. Mater. Interfaces* **6**, 13502 (2014)
54. M. Brahmayya, S.A. Dai, S.Y. Suen, *Sci. Rep.* **7**, 4675 (2017)
55. A. Kulkarni, B. Torok, *Green Chem.* **12**, 875 (2010)
56. G.M. Ziarani, A. Badiiei, N.H. Mohataasham, N. Lashgiri, *J. Chil. Chem. Soc.* **59**, 2271 (2014)
57. H. Sharghi, M. Aberi, J. Aboonajmi, *J. Iran. Chem. Soc.* **13**, 2229 (2016)
58. W. Wu, Y. Guo, X. Xu, Z. Zhou, X. Zhang, B. Wu, W. Yi, *Organ. Chem. Front.* **5**, 1713 (2018)

**Publisher's Note** Springer Nature remains neutral with regard to jurisdictional claims in published maps and institutional affiliations.